Nonlinear analysis of the stick-slip bifurcation in the creep-controlled regime of dry friction

T. Baumberger,[1] C. Caroli,[2] B. Perrin,[1] and O. Ronsin[1]

[1]Laboratoire de Physique de la Matière Condensée de l'Ecole Normale Supérieure, 24 rue Lhomond, 75231 Paris Cedex 05, France

[2]Groupe de Physique des Solides, Universités Paris VI et VII, 2 place Jussieu, 75251 Paris Cedex 05, France

(Received 6 December 1994)

We perform an experimental study of the amplitude and frequency shift of the stick-slip (SS) oscillations of a paper-on-paper block and spring system close to the SS–steady-sliding Hopf bifurcation. The confrontation of the experimental results with a weakly nonlinear analytical analysis of the dynamics and with direct numerical calculations yields very satisfactory agreement with the model of creep-controlled dry friction proposed by Heslot et al. [Phys. Rev. E 49, 4973 (1994)].

PACS number(s): 05.45.+b, 46.30.Pa, 62.20.Hg, 91.30.Px

I. INTRODUCTION

In a recent article [1] we reported the results of an extensive study of the dry friction dynamics of a paper-on-paper block and spring system (Fig. 1), performed over a wide range of relevant control parameters, namely, the imposed velocity V at which the "free" end of the pulling spring is being driven, the spring stiffness K, and the slider mass M. One of the main results emerging from this study is the existence, for V less than a few tens of μm s^{-1}, of low velocity regime in which the friction dynamics of paper exhibits the same characteristic features as already observed on metal [2] and rock [3] systems. This strongly suggests that, in this regime, the nature of the dynamics is material independent and thus susceptible to a generic description. Its main features can be summarized as follows.

(i) It is in this small-V range that the dynamic friction coefficient μ_d, measured in the steady-sliding regime, exhibits velocity weakening. It is well fitted by the functional form

$$\mu_d(V) = a_v - b_v \ln V \ . \tag{1}$$

Here and in all the following velocities and times will be understood to be respectively expressed in μm/s and s. Thus lengths are expressed in μm.

(ii) On the other hand, due to plastic aging of the microcontacts under the normal load [4], the static friction coefficient μ_s increases with the time of the stick t_{st} as

$$\mu_s(t_{st}) \approx a_s + b_s \ln(t_{st}) \tag{2}$$
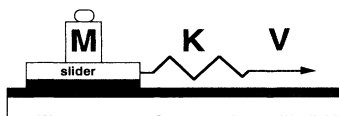
and it is found [1,3] that

FIG. 1. Schematic block and spring arrangement. The mass of the slider is M. The stiffness of the spring is K and its "free" end is driven at constant velocity V.

$$b_s = b_v \ . \tag{3}$$

This leads to defining a characteristic "memory" length [5] D_0—found to lie in the micrometer range—such that

$$\mu_s(\tau) = \mu_d(D_0/\tau) \ . \tag{4}$$

(iii) The sliding motion changes from oscillatory (the so-called stick-slip oscillations) at low spring stiffnesses to steady sliding at large K. The bifurcation between these two regimes shows the qualitative features of a direct (supercritical) Hopf bifurcation controlled, at constant V, by the ratio K/M of the stiffness K and the slider mass M (Fig. 2).

(iv) Once the system is rapidly loaded to a level $\mu_{in} < \mu_s$, pulling then being stopped, the shear stress is observed to relax via a slow nonexponential creeplike motion, the amplitude of which increases as μ_{in} ap-
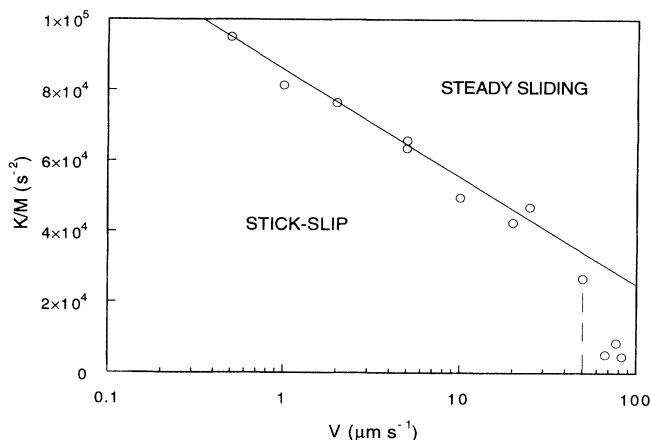

FIG. 2. Phase diagram in control parameter space $(V, K/M)$. Circles indicate the location of the bifurcation from stick-slip to steady sliding. The straight full line corresponds to a logarithmic fit of the data in the creep-dominated regime. For driving velocities $V \gtrsim 50 \ \mu$m s^{-1}, the data markedly deviate from this line, indicating the crossover to the inertia-dominated regime (see Ref. [1]) symbolized by a dashed line.

proaches μ_s from below. The same phenomenon gives rise, in the stick-slip (SS) regime, to an imperfect stick (a slow creep accelerating up until the system crosses over to a rapid inertial slip).

These results have led us [1] to propose a heuristic model borrowing from the ideas put forth in the pioneering work of rock mechanicians [6]. It involves two dynamical variables: a phenomenological contact age Φ, defined so as to account for the idea that the memory length D_0 is the average sliding distance for a given set of contacts to break and be replaced by a fresh, "young" one—Φ therefore depends on the slider dynamical history—and the position $x(t)$ along the pulling direction of the slider center of the mass, assumed to undergo a noise-activated creep motion in an effective pinning potential resulting from the random locking of the surface asperities of the slider by the track ones. The height of the corresponding potential barriers is assumed to increase with the contact age Φ according to a law that is deduced from the measured $\mu_d(V)$.

We have shown that the predictions that can be deduced from this model about the position of the SS–steady-sliding Hopf bifurcation line in the $(K/M, V)$ space and the space period of the relaxing oscillations following velocity perturbations in the steady regime are compatible with our experimental results, while leading us to modify expression (1) into

$$\mu_d(V) = m_0 + m_1 \ln V + m_2 (\ln V)^2 . \tag{5}$$

In such a situation, and given the quite drastic simplifications implicit in our model—in particular the assumed reducibility of the elastic slider dynamics to a one degree of freedom description—it is of course desirable to get independent checks of the validity of our framework by comparing further predictions with measured dynamical characteristics.

From this perspective, we report in this article the results of the study of the SS–steady-sliding bifurcation in the weakly nonlinear regime. We study experimentally the SS amplitude and frequency shift close to the bifurcation, which is shown to be, as already suspected, a direct Hopf one. We then compare these results with the predictions obtained from our model. We find the comparison to yield very good agreement, thus providing a much firmer basis to our proposed description of creep-controlled dry friction.

II. EXPERIMENT

The experimental setup has been described in Ref. [1]. The system consists of a spring-slider arrangement with a paper-on-paper interface (Fig. 1). The key interest of this model system, involving a nonstandard material, is the high regularity and reproducibility of its dynamic behavior.

The data reported here correspond to spring stiffnesses K ranging between 10^4 and 2×10^5 N m^{-1}, masses of the slider M between 0.3 and 3 kg, and driving velocities V between 0.2 and 50 μm s^{-1}; this upper limit roughly marks the crossover to an inertia-dominated regime [1] (see Fig. 2). The spring elongation is measured within

5×10^{-2} μm using an eddy current displacement gauge. The signal of the transducer is monitored on a numerical oscilloscope and a spectrum analyzer with averaging facilities.

In order to analyze the nonlinear behavior of the system close to the bifurcation, we measure the amplitude and the frequency of the stick-slip steady oscillations. As a complement to our previous study of the linear behavior, we also measure the decay time of transient oscillations following a velocity perturbation in the steady-sliding regime.

The main source of uncertainty of these measurements is the "noise" of the system, which originates from interface roughness. Qualitatively, one may distinguish between the effects of large-scale inhomogeneities of the track profile, which result in a small drift of the position of the bifurcation and that of small-scale roughness, which results, close to the bifurcation in the creep regime, in a narrow-band noise centered at a frequency $\sim V/D_0$ [7]. The corresponding noise amplitude, which gives a lower limit of the oscillation amplitude when tuning the control parameter into the steady-sliding regime, is typically on the order of 0.1 μm. This results in a blurring of the onset of the stick-slip regime, which limits the experimental accuracy close to threshold.

In order to obtain data over a significative range of amplitude, we have therefore been led to extend our measurements to large amplitude oscillations (typically 5 μm). Far from threshold, these develop a markedly nonsinusoidal character up to a ratio of the first harmonic amplitude to the fundamental of 1:2. In these conditions, the analytic predictions of the model, based on a small amplitude asymptotic expansion of the dynamic equations, cannot be valid over the whole span of experimental control parameters. Hence we have complemented the analytic calculation by a numerical resolution of the dynamic equations using either a fourth-order Runge-Kutta procedure or an adaptive step-size fifth-order Cash-Karp Runge-Kutta procedure [8] when the strong asymmetry of the stick-slip solution makes it more suitable.

We now turn towards the experimental results, which will be compared with theoretical predictions in Sec. IV. The relevant control parameter in the creep regime is K/M or, equivalently, the dimensionless number $\chi = KD_0/Mg$. The distance to the bifurcation line $\chi_c(V)$ on a path at constant velocity V in parameter space is thus quantified by $\kappa = (1 - \chi/\chi_c)$, defined so that stick-slip occurs when $\kappa > 0$ and steady sliding when $\kappa < 0$. The results are conveniently expressed in an adimensional form, using D_0 as a length scale and the creep time D_0/V as a time scale. We define the "amplitude" ξ as half the peak-to-peak amplitude of the spring oscillations in the stick-slip regime, divided by D_0. The reduced frequency shift $\delta\Omega/\Omega_c = (\Omega - \Omega_c)/\Omega_c$ is defined by reference to the value Ω_c of the pulsation at threshold and τ is the exponential decay time of relaxation oscillations in the steady-sliding regime, divided by D_0/V. Anticipating the results of the next section, we have plotted $\tau^{-1}(\kappa)$, $\xi^2(\kappa)$, and $\delta\Omega(\kappa)$ for a given value of V, namely, 10 μm s^{-1}. The results are shown in Figs. 4, 5, and 6, respectively.

III. WEAKLY NONLINEAR BIFURCATION ANALYSIS

As explained in detail in Ref. [1], in the creep-controlled regime where the motion of the slider center of mass occurs via noise-activated jumps over the age-dependent barriers of the effective pinning potential biased by the pulling force, our dynamical model reduces to

$$\frac{K}{Mg}(Vt - x) = \mu_d \left[\frac{D_0}{\Phi} \right] + A \ln \left[\frac{\dot{x}\Phi}{D_0} \right] , \tag{6}$$

$$\dot{\Phi} = 1 - \frac{\dot{x}\Phi}{D_0} , \tag{7}$$

with $x(t)$ the position of the center of mass and Φ the contact age. The constant $A = 2N_{cr}RT/Mga$ is proportional to the amplitude of the noise, here assumed to be of thermal origin. a is the space period of the pinning potential and N_{cr} the number of moles of material involved in the creep process. In the steady-sliding regime

$$x = x_0(t) = Vt + \Delta x_{st} , \tag{8}$$

$$\Phi = \Phi_0 = D_0/V , \tag{9}$$

with

$$-K\Delta x_{st} = Mg\mu_d(V) . \tag{10}$$

We perform the weakly nonlinear analysis of the bifurcation towards the stick-slip regime with the help of a standard multiscale expansion. Namely, we set

$$\delta x = x - x_0 = \sum_{n=1}^{+\infty} \varepsilon^n X_n(t, T) , \tag{11}$$

$$\delta\Phi = \Phi - \Phi_0 = \sum_{n=1}^{+\infty} \varepsilon^n \Phi_n(t, T) , \tag{12}$$

where the small expansion parameter, which measures the distance from the bifurcation line $\chi = \chi_c(V)$, is defined as

$$\varepsilon = \left[\frac{\delta\chi}{\chi_c(V)} \right]^{1/2} = |\kappa|^{1/2} , \quad \delta\chi = \chi - \chi_c(V) \tag{13}$$

and the slow time variable

$$T = \varepsilon^2 t , \tag{14}$$

where the ε^2 dependence is inferred from the fact that the linear stability analysis (see below and Ref. [1]) yields for the characteristic oscillation frequency close to the bifurcation $\Omega = \Omega_c(1 + \delta\Omega)$ with $\delta\Omega \sim \delta\chi$. We define dimensionless variables and parameters by

$$\bar{x} = \frac{x}{D_0} , \quad \bar{t} = \frac{tV}{D_0} , \quad \bar{\Phi} = \frac{\Phi V}{D_0} \tag{15}$$

and will, from now on, drop the tildes on reduced variables.

Using $\partial/\partial t \to \partial/\partial t + \varepsilon^2 \partial/\partial T$ and plugging expressions (11) and (12) into Eqs. (6) and (7), we obtain (i) order ε,

$$\bar{L}\left[\frac{\partial}{\partial t} \right] \begin{bmatrix} X_1 \\ \Phi_1 \end{bmatrix} = \begin{bmatrix} \chi_c & -A\frac{\partial}{\partial t} - \mu_1 \\ \frac{\partial}{\partial t} & \frac{\partial}{\partial t} + 1 \end{bmatrix} \begin{bmatrix} X_1 \\ \Phi_1 \end{bmatrix} = 0 , \tag{16}$$

from which

$$\begin{bmatrix} X_1 \\ \Phi_1 \end{bmatrix} = \alpha(t) \begin{bmatrix} u \\ 1 \end{bmatrix} e^{i\Omega_c t} + \text{c.c.} , \tag{17}$$

where

$$\chi_c(V) = -\mu_1 \equiv - \left[\frac{d\mu_d(V)}{d(\ln V)} \right] , \tag{18a}$$

$$\Omega_c^2 = \chi_c/A , \tag{18b}$$

and

$$u = -[1 + (i\Omega_c)^{-1}] ; \tag{18c}$$

(ii) order ε^2,

$$\begin{bmatrix} X_2 \\ \Phi_2 \end{bmatrix} = \begin{bmatrix} -\frac{\mu_1 + \mu_2}{2}\Phi_1^2 + \frac{A}{2}\left[\frac{\partial\Phi_1}{\partial t} \right]^2 \\ -\Phi_1 \frac{\partial X_1}{\partial t} \end{bmatrix} \tag{19}$$

with

$$\mu_n = \frac{d^n \mu_d(V)}{d(\ln V)^n} , \tag{20}$$

from which Eq. (17) immediately yields

$$\begin{bmatrix} X_2 \\ \Phi_2 \end{bmatrix} = \begin{bmatrix} C_{22} \\ D_{22} \end{bmatrix} e^{2i\Omega_c t} + \text{c.c.} + \begin{bmatrix} C_{20} \\ D_{20} \end{bmatrix} \tag{21}$$

with

$$\begin{bmatrix} C_{22} \\ D_{22} \end{bmatrix} = \alpha(T)^2 [\bar{\bar{L}}(2i\Omega_c)]^{-1} \begin{bmatrix} \frac{\mu_2}{2} \\ -i\Omega_c u \end{bmatrix} , \tag{22a}$$

$$\begin{bmatrix} C_{20} \\ D_{20} \end{bmatrix} = |\alpha(T)|^2 [\bar{\bar{L}}(0)]^{-1} \begin{bmatrix} -2\mu_1 - \mu_2 \\ -i\Omega_c(u - u^*) \end{bmatrix} ; \tag{22b}$$

and (iii) order ε^3, for which the equation for X_3 and Φ_3 can be written as

$$\bar{L}\left[\frac{\partial}{\partial t} \right] \begin{bmatrix} X_3 \\ \Phi_3 \end{bmatrix} = \begin{bmatrix} \lambda \\ \nu \end{bmatrix} e^{i\Omega_c t} + \text{c.c.}$$

$$+ (\text{nonresonant terms}) , \tag{23}$$

where

$$\lambda = \chi_c \alpha u + A\frac{\partial\alpha}{\partial T} + \alpha|\alpha|^2 \left[\mu_1(1 - i\Omega_c) + \frac{3\mu_2 + \mu_3}{2} \right]$$

$$- \alpha^* D_{22}(3\mu_1 + \mu_2) - \alpha D_{20}(\mu_1 + \mu_2) , \tag{24a}$$

$$\nu = -(u + 1)\frac{\partial\alpha}{\partial T} + i\Omega_c \alpha^*(u^* D_{22} - 2C_{22}) - i\Omega_c \alpha u D_{20} , \tag{24b}$$

and nonresonant terms refers to those with frequency $\pm 3\Omega_c$, which do not resonate with the eigenmodes $(\pm \Omega_c)$ of $\overline{\overline{L}}$.

In order for Eq. (23) to be solvable it must satisfy the Fredholm condition, which reduces here to

$$\frac{\lambda}{v} = \frac{L_{12}(i\Omega_c)}{L_{22}(i\Omega_c)} = \frac{L_{11}(i\Omega_c)}{L_{21}(i\Omega_c)} , \qquad (25)$$

i.e., to

$$\lambda + i\Omega_c A v = 0 . \qquad (26)$$

Using Eqs. (22), Eq. (26) can be written as

$$2A\frac{\partial \alpha}{\partial T} + (\mu_1 + iA\Omega_c)\alpha + (\gamma_3 + i\delta_3)|\alpha|^2 \alpha = 0 , \qquad (27)$$

where

$$\gamma_3 = \frac{\mu_2 + \mu_3}{2} , \quad \delta_3 = -\frac{\Omega_c}{3}\left[\mu_1 + \mu_2 + \frac{\mu_2^2}{\mu_1}\right] - \frac{\mu_1}{3\Omega_c} . \qquad (28)$$

The solution of Eq. (22) has the form

$$\alpha(T) = \alpha_0 e^{i\eta T} \qquad (29a)$$

with

$$\alpha_0 = -\frac{2\mu_1}{\mu_2 + \mu_3} = \frac{2\chi_c}{\mu_2 + \mu_3} , \qquad (29b)$$

$$\eta = -\frac{\Omega_c}{2}\left[1 + \frac{\delta_3}{\Omega_c}\frac{\alpha_0^2}{A}\right] , \qquad (29c)$$

that is, finally,

$$\delta X^{(1)} \equiv \varepsilon X_1(t,T) = \xi \cos[(\Omega_c + \delta\Omega)t + \psi] , \qquad (30)$$

where the amplitude ξ and the frequency shift $\delta\Omega$ of the stick-slip oscillation are given by

$$\xi^2 = \kappa \frac{8(\chi_c + A)}{(\mu_2 + \mu_3)} , \qquad (31)$$

$$\delta\Omega = -\kappa\frac{\Omega_c}{2}\left\{1 + \frac{2\chi_c\Omega_c^2}{3(\mu_2 + \mu_3)}\right.$$

$$\left. \times\left[1 + \frac{1}{\Omega_c^2} + \frac{\mu_2}{\mu_1} + \left[\frac{\mu_2}{\mu_1}\right]^2\right]\right\} . \qquad (32)$$

IV. COMPARISON WITH EXPERIMENTAL RESULTS

A key parameter for the quantitative analysis of the model is the memory length D_0, which is determined from the experimental friction laws (1) and (2):

$$D_0 = \exp\left[\frac{a_v - a_s}{b_v}\right] \approx 1 \ \mu\text{m} . \qquad (33)$$

Since the numerical evaluation of D_0 involves an exponentiation, the uncertainty of its value is large and can be roughly estimated as $\pm 0.3 \ \mu$m. In the following, we will make use of the value $D_0 = 1 \ \mu$m.
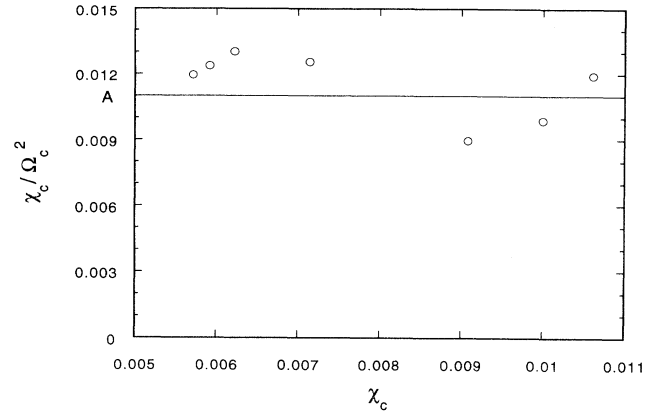

FIG. 3. Plot of the ratio χ_c/Ω_c^2 versus χ_c for data at various V and M. The solid line is a fit with constant parameter A (see the text).

The value of the parameter A [9] has been determined from the ratio χ_c/Ω_c^2 at various velocities V, the constant K and hence various masses M. The data shown in Fig. 3 are well fitted to the constant A value

$$A = 1.1 \times 10^{-2} \pm 2 \times 10^{-3} .$$

We now turn to the determination of the dynamic friction coefficient $\mu_d(V)$. The comparison of experimental results with the predictions of our dynamical model requires the knowledge of the function $\mu_d(V)$. This we deduce from measurements of friction coefficients and of the position of the bifurcation line as follows.

(i) The value of $b_v = b_s$ as obtained from (1) and (2) is $b_v = b_s = 1.3 \times 10^{-2} \pm 1 \times 10^{-3}$ and provides a first approximation of the mean value $\langle\mu_1\rangle$ of $\mu_1(V)$ over three decades of V, namely,

$$\langle\mu_1\rangle = -b_v \approx -1.3 \times 10^{-2} .$$

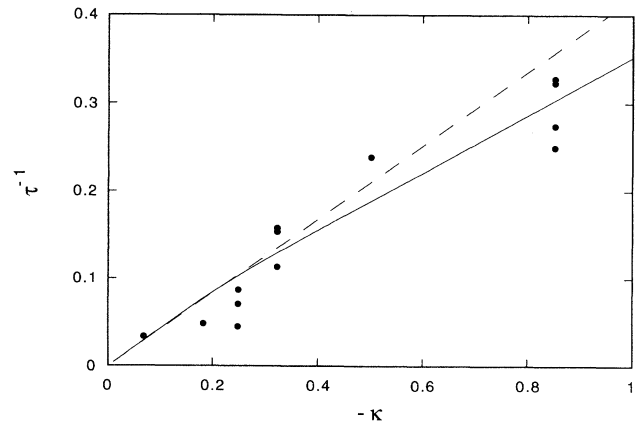(ii) The mean experimental value of $d\chi_c/d(\ln V)$ is

FIG. 4. Plot of the dimensionless decay rate τ^{-1} versus the control parameter κ at given $V = 10 \ \mu$m s^{-1}. The dashed straight line corresponds to the analytical linear prediction of Eq. (34). The solid curve corresponds to the numerical resolution of the dynamic equations.
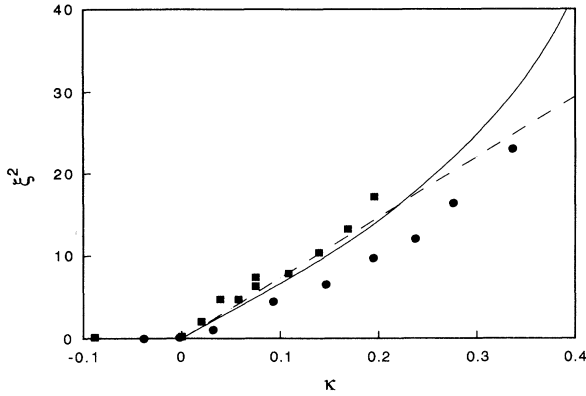
FIG. 5. Plot of the dimensionless squared amplitude ξ^2 versus κ for two sets of data at $V = 10 \ \mu\mathrm{m\,s}^{-1}$ (circles and squares). The dashed straight line corresponds to the analytical prediction of Eq. (31) and the solid curve to the numerical resolution of the dynamic equations.
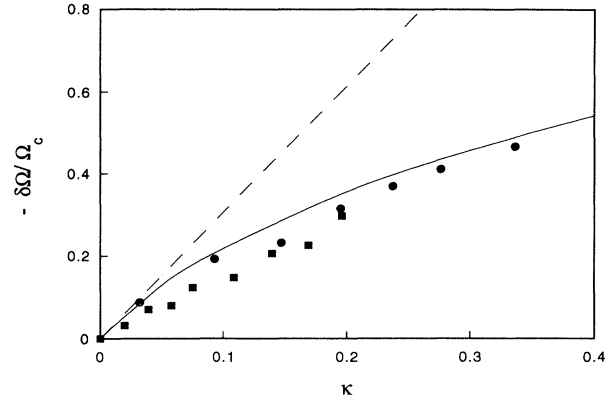

FIG. 6. Plot of the dimensionless frequency shift $-\delta\Omega/\Omega_c$ versus κ for the same set of data as in Fig. 5. The dashed straight line corresponds to the analytical prediction of Eq. (32) and the solid curve to the numerical resolution of the dynamic equations.

$2 \times 10^{-3} \pm 5 \times 10^{-4}$; hence the mean value $\langle \mu_2 \rangle$ of $\mu_2(V)$ is

$$\langle \mu_2 \rangle \approx 2 \times 10^{-3} \ .$$

(iii) A quadratic fit of $\chi_c(\ln V)$ gives a value of 2×10^{-4} for m_3, well below the dispersion and the accuracy of the experimental data; hence a conservative value for the mean value $\langle \mu_3 \rangle$ of $\mu_3(V)$ is

$$\langle \mu_3 \rangle = 0 \ .$$

In view of the relatively high uncertainties of the values of the key parameters D_0, A, $\langle \mu_1 \rangle$, $\langle \mu_2 \rangle$, and $\langle \mu_3 \rangle$, it seems reasonable to test the predictive nonlinear analysis of the model with this set of values, without further adjustment. Since $\langle \mu_2 \rangle \ll \langle \mu_1 \rangle$, we can finally use for $\mu_d(V)$ expression (5) with $m_1 = \langle \mu_1 \rangle$ and $m_2 = \langle \mu_1 \rangle$; as it appears in Eqs. (6) and (7), $m_0 \approx 0.4$ only acts to shift the mean slider position and has no effect on the dynamics in the creep regime.

As a first test, we have analyzed the behavior of the relaxation time $\tau(\kappa)$ with $\kappa < 0$. The linear analysis [Eq. (16)] yields

$$\tau^{-1} = -\frac{\chi_c}{2A}\kappa \ . \tag{34}$$

This is represented by the dashed line of Fig. 4, but, as already mentioned, since our data range over values of the reduced parameter $|\kappa|$ as high as 0.8, it is necessary to use a numerical resolution of the dynamic equations (6) and (7). The calculated curve (full line in Fig. 4) is in good agreement with the data over the whole range of $|\kappa|$. The same agreement is found for values of V ranging from 0.25 to 10 $\mu\mathrm{m\,s}^{-1}$.

We then test the data $\xi^2(\kappa)$ and $(\delta\Omega/\Omega_c)(\kappa)$ for $\kappa > 0$ against expressions (31) and (32). The corresponding graphs, for $V = 10 \ \mu\mathrm{m\,s}^{-1}$, are plotted as dashed lines in Figs. 5 and 6; full lines are the results of the numerical integration of (6) and (7). It is seen that while the weakly nonlinear analytic result provides a good description of amplitude data up to values of κ of order 0.2, deviations due to higher-order nonlinear effects are much more important for the frequency shift. Again, the agreement appears quite satisfactory; the same order of agreement is found for driving velocities V down to 1 $\mu\mathrm{m\,s}^{-1}$.

In conclusion, the present analysis provides two independent checks of the validity of the dynamic model that we have proposed to describe stick-slip oscillations in the creep-controlled regime. In view of the crudeness of our approach, which reduces the description of the dynamics of the elastic slider to a single degree of freedom, this result may seem surprising. We think that it strongly suggests that the coherence length, which measures the average size of collective events of rupture of the randomly distributed microcontacts, is comparable, in our system, to the sample size [10]. The relevance of our description thus being established, at least for our experimental system, on a quite firm basis, it now seems justified to use it to explore the low velocity, fully nonlinear dynamics, in the spirit of the work of Gu and Wong [11] on rock friction, as well as to try to characterize in more detail the crossover to the inertia controlled regime.

[1] F. Heslot, T. Baumberger, B. Perrin, B. Caroli, and C. Caroli, Phys. Rev. E **49**, 4973 (1994).

[2] E. Rabinowicz, *Friction and Wear of Materials* (Wiley, New York, 1965).

[3] C. H. Scholz, *The Mechanics of Earthquake and Faulting* (Cambridge University Press, Cambridge, England, 1990), Chap. 2, and references therein.

[4] F. P. Bowden and D. Tabor, *Friction and Lubrication of*

Solids (Clarendon, Oxford, 1950).

[5] J. H. Dieterich, J. Geophys. Res. **84**, 2161 (1979).

[6] A. Ruina, J. Geophys. Res. **88**, 10 359 (1983); J. R. Rice and A. Ruina, J. Appl. Mech. **50**, 343 (1983).

[7] T. Baumberger, O. Ronsin, F. Heslot, and B. Perrin, Bull. Soc. Fr. Phys. **94**, 3 (1994).

[8] W. H. Press, S. A. Teukolsky, W. T. Vetterling, and B. P. Flannery, *Numerical Recipies in C*, 2nd ed. (Cambridge University Press, Cambridge, England, 1992).

[9] Note that A, as here defined, contains factor $1/Mg$ as compared with the quantity called A in Ref. [1].

[10] T. Baumberger and C. Caroli, Comments Condens. Matter Phys. (to be published).

[11] Y. Gu and T.-F. Wong, in *Non-Linear Dynamics and Predictability of Geophysical Phenomena*, edited by A. Gabrielov and W. Neuman, Geophysical Monograph No. 83 (AGU, Washington, DC, 1994).